Single W-boson Production at Linear Colliders

E.E. Boos, M.N. Dubinin
Institute of Nuclear Physics, Moscow State University
119899 Moscow, Russia

Abstract

The process of single W boson production at the energies of Next Linear Colliders is considered. We discuss in details the contributions from s and t channel diagrams, technical aspects of the complete tree level calculation with a finite W width, and the quark mass effects.

The process of single W-boson production $e^+e^- \to e^-\bar{\nu}_e u\bar{d}$ ("CC20 process" in the four fermion channels classification of [1]) has been considered in details both from experimental and theoretical viewpoints. From the experimental point of view this process gives an important contribution to the cross section of W^+W^- pair production as well as to the rate of single W production, when the initial electron (positron) goes to the beam pipe. At the same time CC20 process represents the main background to signals of new physics (especially R-parity conserving or violating SUSY processes) and provides a strong restrictions on the anomalous three vector boson couplings $WW\gamma$, WWZ. From the theoretical point of view the cross section of $e^+e^- \to e^-\bar{\nu}_e u\bar{d}$ channel is sensitive to a huge gauge cancellations between the individual diagrams from the complete tree level set, and the singularity of the amplitude at zero scattering angle of the electron, when the treatment of finite W-boson width and finite electron mass is delicate and needs much care [2, 3]. It will be also pointed out that the ISR corrections to CC20 process should be calculated with different characteristic energy scales for the two gauge invariant subsets of contributing diagrams.

The set of 20 diagrams of the process CC20 can be divided into two gauge invariant (with respect to the SM gauge group) subsets of 10 t-channel (Fig.1) and 10 s-channel diagrams (Fig.2). If the lepton and the corresponding neutrino in the final state of $e^+e^- \to e^-\bar{\nu}_e u\bar{d}$ are replaced by the muon or tau with corresponding neutrino, only 10 s-channel diagrams remain and represent the analogous μ and τ CC10 channels. Electron scattering at zero angle from the t-channel subset is absent in these channels. It is a simple proof that both CC10 channels are gauge invariant. The less trivial statement is that these two CC10 classes are the minimal gauge invariant SM subsets. In fact it follows from the general theorem proved recently in [4].

Our calculation of the total rate have been performed by means of *CompHEP* package [5]. The squared amplitude with finite electron mass $m_e = 0.511$ MeV have been used in this calculation, so the forward electron pole is regulated by the kinematical cutoff $t_{max} = -m_e^2(M^2/s)^2$, where M denotes an invariant mass scale for the $\bar{\nu}_e u\bar{d}$ system (see Fig.3). Results of *CompHEP* calculation are shown in Table 1 together with the results of other groups obtained by means of *grc4f* [6], *KORALW* [7] and *WPHACT* [8] generators. *grc4f* and *WPHACT* generators also use the finite fermion mass amplitude and *KORALW* contains *grc4f* matrix element inside. Their phase space intergation routines are different. Good agreement between the three generators (*CompHEP*, *grc4f*, *WPHACT*) is observed while *KORALW* results obtained for $\sqrt{s}$ =500 GeV are somewhat smaller. The agreement of cross sections is not trivial since *CompHEP*, *grc4f* and *WPHACT* are using different prescriptions for the insertion of Breit-Wigner propagator into the complete tree level amplitude.

In the 'overall' prescription (also called the 'preserved gauge' scheme) used by *CompHEP* and *WPHACT*, resonant and nonresonant parts of the amplitude

$$\frac{a_\mu}{p_W^2 - m_W^2} + b_\mu \tag{1}$$

are squared, summed and then multiplied by the 'overall' factor

$$\frac{(p_W^2 - m_W^2)^2}{(p_W^2 - m_W^2)^2 + m_W^2\Gamma_W^2} \tag{2}$$

In *CompHEP* the number of overall factors is equal to the number of W propagators in the diagram set, and the prescription has beed applied to two gauge invariant CC10 subsets separately in order to avoid an artificial suppression of CC10-t part in the phase space region close to the position of the second W pole from the CC10-s part.

grc4f and *KORALW* prescriptions [2] are based on the gauge-invariance motivated redefinition of the leptonic tensor $L_{\mu\nu}$ [2, 10] for the t-channel subset

$$L_{\mu\nu} \quad = \quad 2(p_\mu p'_\nu + p_\nu p'_\mu) + q^2\, g_{\mu\nu}$$

to the form

$$L'_{\mu\nu} \quad = \quad 4(p_\mu - \frac{p_0}{q_0}\, q_\mu)(p_\nu - \frac{p_0}{q_0}\, q_\nu) + q^2\, g_{\mu\nu}$$

Unadequate treatment of finite W width violates the gauge cancellation of the double pole $1/t^2 = 1/(p'_e - p_e)^4$ for t-channel gamma and leads to nonunitary (powerlike) energy behaviour of the amplitude. The overall prescription or the redifinition $L_{\mu\nu} \to L'_{\mu\nu}$ ensures a numerically stable cancellation of the double pole to the single one $1/t$. This cancellation in the preserved gauge scheme used in *CompHEP* can be explicitly demonstrated if we plot the distribution in $log_{10}|t|$ (see Fig.3 (1)). Flat part of the distribution is related to the unitary behaviour $d\sigma/dt \sim 1/t$. In the framework of the equivalent gamma approach this behaviour corresponds to the canonical Wieszacker-Williams approximation. The falldown of the distribution starting at about $log_{10}|t| \sim$ -6-7 reflects an improved Wieszacker-Williams behaviour [11] The W peak is observed in Fig.2 at $log_{10}|t| \sim 4$. [1]

We present the results of *CompHEP* calculation for contributions of separately taken s-channel and t-channel subsets to the total rate, as well as their interference contribution, at various energies in Table 2. Quark phase space cuts $E_q > 3$ GeV, $M_{ud} > 5$ GeV and/or lepton phase space cut $\cos\vartheta_e > 0.997$ are imposed. From Table 2 and Fig.4 one can see that the contribution of t-channel subset increases rapidly with energy while the s-channel cross section goes down and becomes smaller than the t-channel at the energy about 320 GeV. The s-t interference is extremely small in all the energy range under consideration (100 GeV - 1 TeV). At LEP2 energies the single W production process is less important than the W^+W^- pair production, but at the energies of LC single W creation plays the dominant role.

Table 3 contains the cross section values at different energies without cuts, when the t-channel gamma pole and the t-channel u/d quark poles in the ladder diagram are regulated by the electron and light quark masses $m_u = 5$ MeV, $m_d = 10$ MeV. It is important to point out that at nonzero electron mass the finite numerical result exists even for massless quarks. If we denote the minimal quark momentum fraction by x_{min}

$$x_{min} = \frac{(m_u + m_d + m_e)^2}{s}$$

the maximal gamma momentum transferred

$$t_{max} = -m_e^2\, \frac{x_{min}^2}{1 - x_{min}}$$

and the kinematical cutoff near the pole still exists at $m_u = m_d = 0$. It is important to understand a role of the multiperipheral diagrams in the CC10 t-channel subset. However, it makes no sense to compute straightfrwardly a contribution from that diagrams because they do not form a gauge invariant class. But one can get an information about a size of the multiperipheral diagrams contribution by calculating a dependence of the cross section on a quark mass. These diagrams represent the only production mechanism that could depend significantly on the values of quark masses. We calculated the cross section dependence on the quark mass $m_q = m_u = m_d$ changing from 1 MeV to 100 MeV (see Table 4 and Fig.4). The total rate decreases from 1442 fb to 1414 fb, so rather weak but distinct dependence on the quark mass takes place. Therefore one can expect a rather small 'resolved photon' contribution to CC20 process rate. Instructive comparison can be done with the case of resolved photon contribution to the single W production process at HERA (ep collisions), where the latter is estimated to be of order 10-15% of the total W rate [12]. In the case of ep collisions the most important t-channel diagram topology (see diagram 7 in Fig.1) contains a quark line and t-channel gamma, giving rise to

[1] Detailed comparison of the same kind as indicated above at LEP2 energies $\sqrt{s} = 183$ and 190 GeV can be found in [9].

potentially high resolved cross section $\gamma^* q \to hadrons$. In the case of e^+e^- collisions this contribution is absent and only subleading multiperipheral topologies (see diagrams 2,3 in Fig.1) could give the resolved $\gamma^* q \to hadrons$.

The calculation of initial state radiative corrections (ISR) to CC20 process needs a special care. Two different scales of ISR radiator function should be used for the t and s channel subsets of diagrams. If we take $Q^2 = s$ for s channel and $Q^2 = 0$ for t-channel, the cross section can be calclated as a sum of s-channel contribution with ISR and t-channel contribution without ISR from the Table 2. The same is also true for the value of α_{QED} which should be taken differently for t-channel and s-channel sets. Obviously, the characteristic scale for the t-channel part is $Q^2 = 0$ and therefore one should use 1/137 while a typical scale of the s-channle piece is of the order s and a value of about 1/128 should be used.

The authors are grateful to E. Accomando, A. Ballestrero and G. Passarino for useful discussions and to DESY-Zeuthen TESLA group for the kind hospitality. This work was partly supported by the joint RFBR-DFG grant 99-02-04011.

References

[1] Event generators for WW physics, conveners D. Bardin, R. Kleiss, in: *Physics at LEP2*, ed. by G. Altarelli, T. Sjoestrand, F. Zwirner, CERN report 96-01, 1996, vol.II

[2] Y. Kurihara, D. Perret-Gallix, Y. Shimizu, Phys.Lett. B349 (1995) 367.

[3] W. Beenakker et. al., Nucl.Phys. B500 (1997) 255.
G. Passarino, hep-ph/9810416

[4] E. Boos, T. Ohl, Phys.Rev.Lett. 83 (1999) 480.

[5] E. Boos, M. Dubinin, V. Ilyin, A. Pukhov, V. Savrin, preprint INP MSU 94-36/358, 1994 (hep-ph/9503280)
P. Baikov et.al, in: *Proc.of X Workshop on High Energy Physics and Quantum Field Theory*, ed.by B. Levtchenko, V. Savrin, Moscow, 1996, p.101
A. Pukhov et.al., hep-ph/9908288
see also `http://theory.npi.msu.su/~comphep`

[6] T. Ishikawa, T. Kaneko, K. Kato, S. Kawabata, Y. Shimizu, H. Tanaka, KEK report 92-19, 1993

[7] S. Jadach, W. Placzek, M. Skrzypek, B.F.L. Ward, Z. Was, CERN-TH-98-242, 1998

[8] E. Accomando, A. Ballestrero, Comp.Phys.Comm., 99 (1997) 270.

[9] A. Ballestrero, talk at LEP2 miniworkshop, CERN, 12-13 March 1999

[10] F. Gutbrod, Z. Rek, Z.Phys. C1 (1979) 171.

[11] S. Frixione, M. Mangano, P. Nason, G. Ridolfi, Phys.Lett. B319 (1993) 339.

[12] M.N. Dubinin, H.S. Song, Phys.Rev. D57 (1998) 2927.
U. Baur, J. Vermaseren, D. Zeppenfeld, Nucl.Phys. B375 (1992) 3.

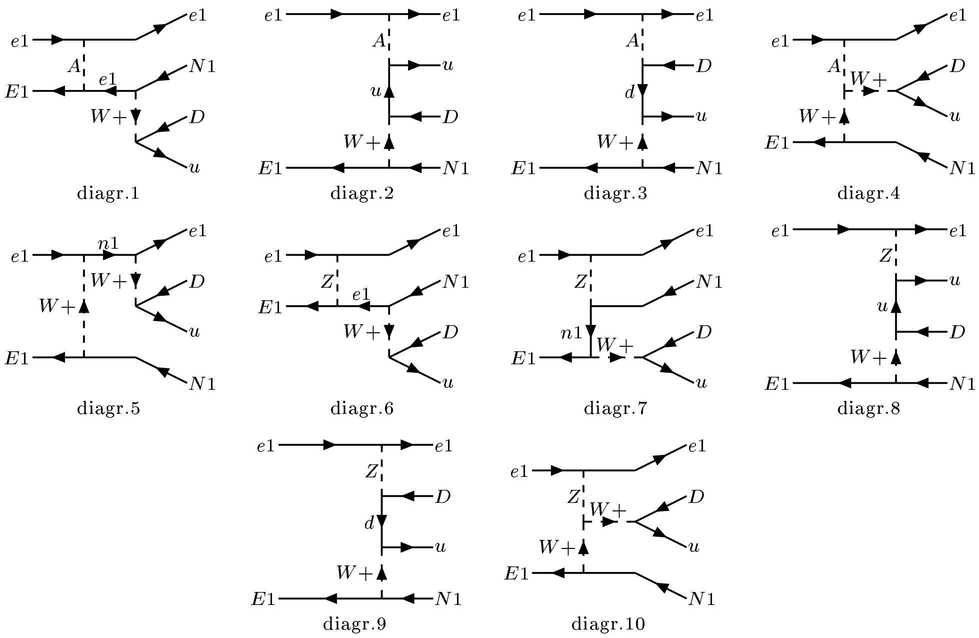

Figure 1: t-channel Feynman diagrams for the process $e^+e^- \to e^-\bar{\nu}_e u\bar{d}$.

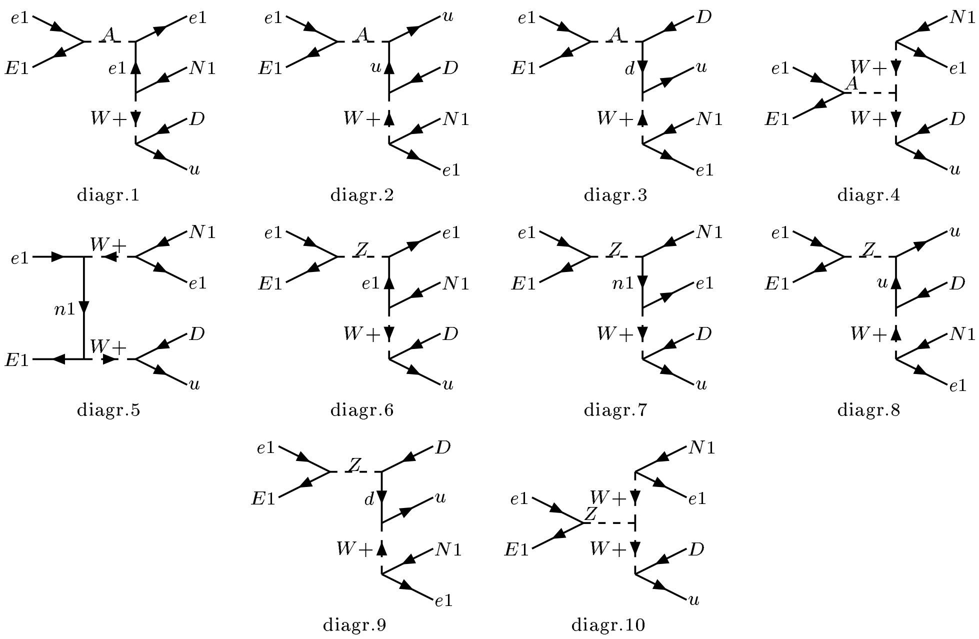

Figure 2: s-channel Feynman diagrams for the process $e^+e^- \to e^-\bar{\nu}_e u\bar{d}$.

	CompHEP	grc4f	KORALW	WPHACT
$\sqrt{s} = 350$ GeV				
q cuts, no ISR	1076(1)	1080(2)		1074(1)
q cuts, with ISR	1039(1)	1040(1)		1038(2)
q, e cuts, no ISR	520(1)	521(1)		512(1)
q, e cuts, with ISR	478(1)	480(1)		479(2)
$\sqrt{s} = 500$ GeV				
q cuts, no ISR	1417(2)	1419(2)	1395(6)	1418(1)
q cuts, with ISR	1357(5)	1359(2)	1336(6)	1358(2)
q, e cuts, no ISR	939(3)	939(1)	909(5)	936(1)
q, e cuts, with ISR	864(9)	874(1)	840(5)	847(2)
$\sqrt{s} = 800$ GeV				
q cuts, no ISR	2140(4)	2146(3)		2138(3)
q cuts, with ISR	2048(4)	2046(3)		2042(2)
q, e cuts, no ISR	1687(4)	1697(2)		1692(3)
q, e cuts, with ISR	1597(3)	1597(2)		1593(2)

Table 1: CompHEP, grc4f, KORALW and WPHACT results for the total cross section of the process $e^+e^- \to e^-\bar{\nu}_e u\bar{d}$ (fb) at $\sqrt{s} = 350$, 500 and 800 GeV. The notation 'q cuts' means partonic level quark cuts $E_q \geq 3$ GeV, $M_{ud} \geq 5$ GeV, 'l cuts' corresponds to $\cos\theta_e \geq 0.997$ One standard deviation error of the last digit is indicated in brackets.

$\sqrt{s}$	$\sigma(CC10-t)$	$\sigma(CC10-s)$	$\sigma(t-s\ interf.)$	σ_{tot}
quark phase space cuts, no ISR				
183	130(0)	655(1)	0.2(0)	785(1)
190	147(0)	680(1)	5(0)	832(1)
350	635(1)	420(1)	21(0)	1076(1)
500	1127(2)	270(0)	19(0)	1417(2)
800	1981(4)	143(0)	16(0)	2140(4)
quark phase space cuts, with ISR				
183	117(0)	566(1)	0.2(0)	683(1)
190	132(0)	603(1)	5(0)	739(1)
350	587(1)	432(1)	20(0)	1039(1)
500	1049(5)	289(0)	19(0)	1357(5)
850	1873(4)	159(0)	16(1)	2048(4)
lepton and quark phase space cuts, no ISR				
183	102(0)	2(0)	0.0(0)	104(0)
190	116(0)	2(0)	0.0(0)	118(0)
350	513(1)	7(0)	0.2(0)	520(1)
500	928(2)	10(0)	0.3(0)	938(2)
800	1671(4)	15(0)	0.4(0)	1686(4)
lepton and quark phase space cuts, with ISR				
183	92(1)	2(0)	0.0(0)	94(1)
190	103(1)	2(0)	0.0(0)	105(1)
350	472(1)	6(0)	0.0(0)	478(1)
500	854(9)	10(0)	0.3(0)	864(9)
800	1581(3)	15(0)	0.4(0)	1596(3)

Table 2: Contributions to the total cross section (in fb) of the CC20 process $e^+e^- \to e^-\bar{\nu}_e u\bar{d}$ from the gauge invariant subsets of t-channel and s-channel diagrams and their interference at the energies of LEP2 and NLC. One standard deviation error of the last digit is indicated in brackets.

$\sqrt{s}$	$\sigma(CC10-t)$	$\sigma(CC10-s)$	$\sigma(t-s\ interf.)$	σ_{tot}
no cuts, no ISR				
183	141(0)	655(1)	0.2(0)	796(1)
190	158(0)	680(1)	5(0)	843(1)
500	1141(2)	271(0)	19(0)	1531(2)
800	2000(6)	143(0)	16(0)	2159(6)

Table 3: Contributions to the total cross section (in fb) of the CC20 process $e^+e^- \to e^-\bar{\nu}_e u\bar{d}$ from the gauge invariant subsets of t-channel and s-channel diagrams and their interference at the energies of LEP2 and NLC. Phase space cuts are not imposed. One standard deviation error of the last digit is indicated in brackets.

m_q (MeV)	$\sigma(CC10-t)$	$\sigma(CC10-s)$	$\sigma(t-s\ interf.)$	σ_{tot}
0	1160(4)	270(0)	20(0)	1450(4)
0.5	1154(3)	270(0)	20(0)	1444(3)
1	1152(3)	270(0)	20(0)	1442(3)
5	1147(2)	270(0)	20(0)	1437(3)
10	1142(2)	270(0)	20(0)	1432(3)
50	1131(2)	270(0)	20(0)	1421(2)
100	1124(2)	270(0)	20(0)	1414(2)

Table 4: The total rate for the process $e^+e^- \to e^-\bar{\nu}_e u\bar{d}$ (fb) at various quark masses.

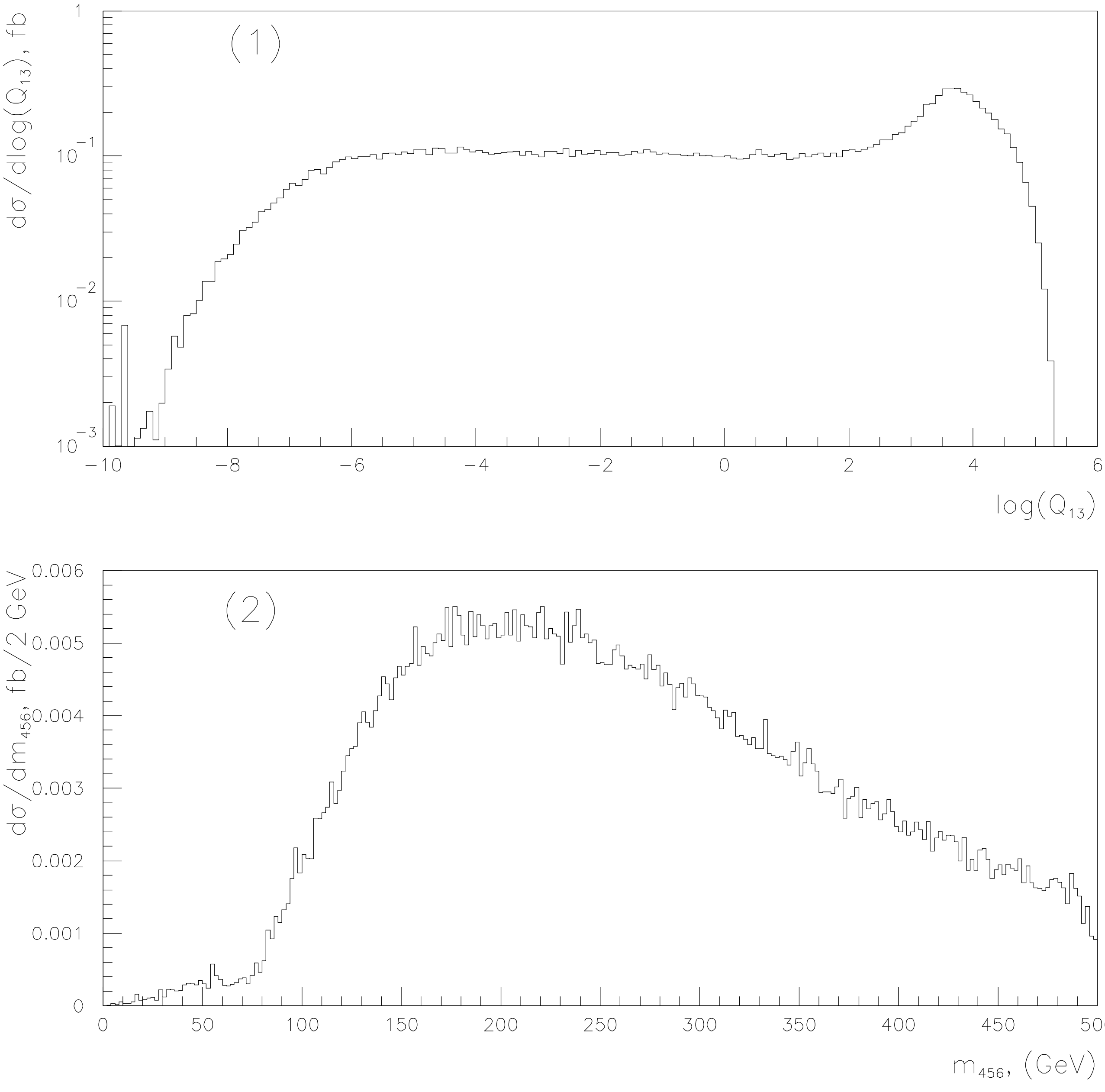

Figure 3: (1)- the distribution of $\log_{10}(Q^2)$, (2) - the $M_{\nu u \bar{d}}$ invariant mass distribution

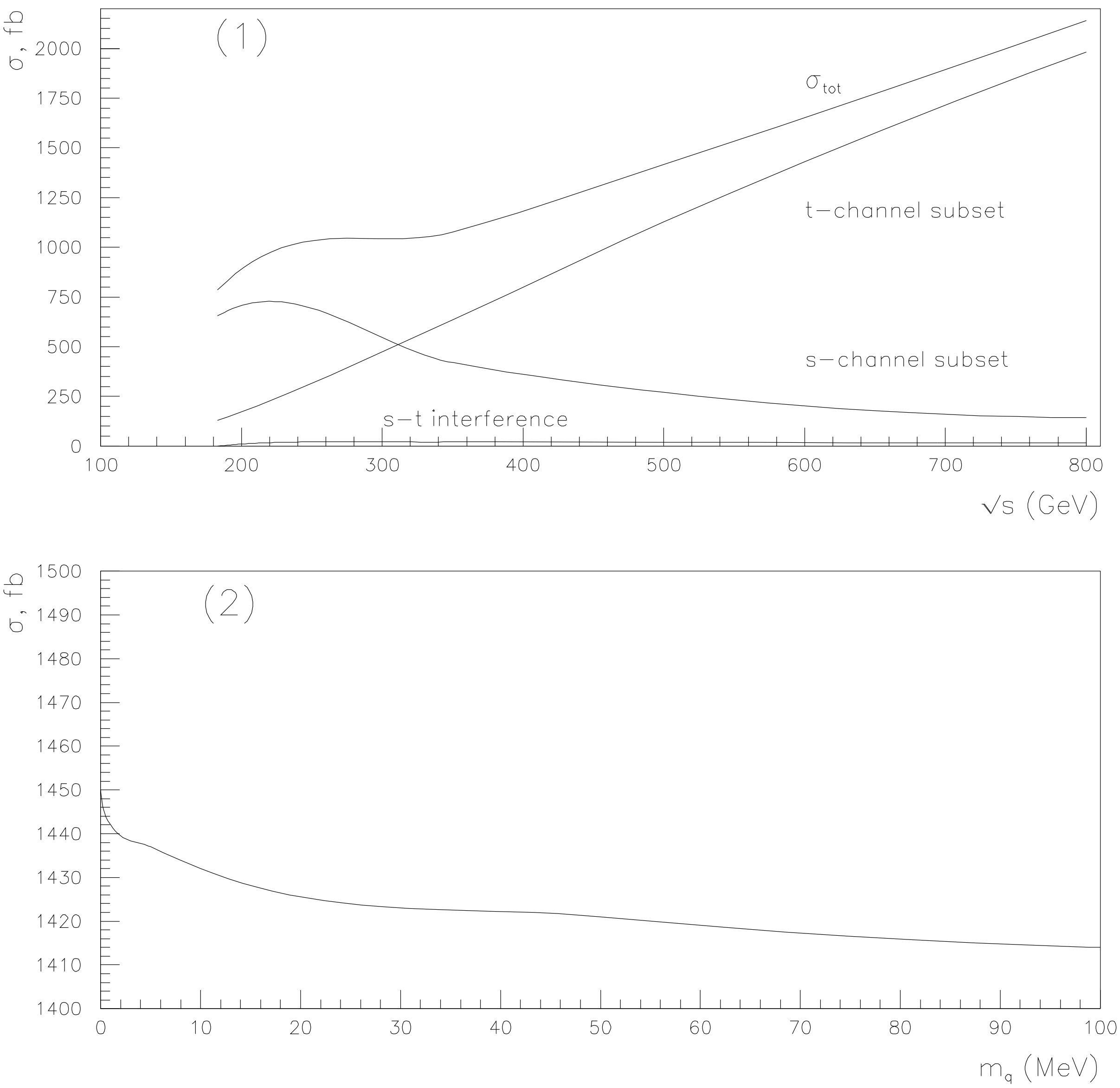

Figure 4: (1)- s and t channel subset contributions to σ_{tot}, (2) - total cross section dependence on the quark mass.